

# Optimal Design of Solar-Aided Hydrogen Production Process Using Molten Salt

Wanrong Wang, Nan Zhang, Jie Li\*

Centre for Process Integration, Department of Chemical Engineering and Analytical Science, The University of Manchester, Manchester M13 9PL, UK  
 jie.li-2@manchester.ac.uk

In this work, a machine-learning based optimisation framework is proposed for optimal design of solar steam methane reforming using molten salt (SSMR-MS) through machine learning techniques. The artificial neural network (ANN) is employed to establish relationships between total annualised cost (TAC), hydrogen production rate and molten salt duty, and independent input variables in SSMR-MS. A hybrid global optimisation algorithm is adopted to solve the developed surrogate model and generate the optimal design. The computational results demonstrate that a significant reduction in TAC by around 15 % can be achieved than the existing SSMR-MS. The lowest Levelised cost of Hydrogen Production (LCHP) is 2.43 \$ kg<sup>-1</sup> which is reduced by around 15 % compared to the existing process with LCHP of 2.85 \$ kg<sup>-1</sup>.

## 1. Introduction

Hydrogen is an important energy carrier in the transportation sector and essential industrial feedstock for petroleum refineries, methanol, and ammonia production. It is anticipated that hydrogen global demand will increase 10-fold by 2050 (Hydrogen Council., 2017). Conventional hydrogen production mainly uses natural gas and oil-based feedstock for steam reforming, which results in considerable greenhouse gas emissions, and consequently contributes to global warming (Voldsund et al., 2016). Therefore, investigation of clean and affordable hydrogen production process using renewable energy sources is crucial (Turner et al., 2008).

Solar energy for hydrogen production has received significant attention in recent years due to its primary abundance as an energy source (Koumi Ngoh et al., 2012). It can be utilised for hydrogen production in three ways: photochemically, thermochemically and electrochemically (Liu et al., 2019). However, the low solar to hydrogen efficiency and instability of solar systems indicate the solar hydrogen production rate is inferior to that of the industrial scale (Liu et al., 2019). To effectively use solar energy for large-scale hydrogen production, solar steam methane reforming using a volumetric receiver reactor (SSMR-VRR), SSMR-MS and solar thermal power generation coupled with water electrolysis (STP-WE) have been developed and evaluated (Likkasit, 2015). The SSMR-MS shows greatest potential due to its unlimited operation hours and lower TAC.

However, no effort has been made for optimal design of SSMR-MS process to reduce TAC and CO<sub>2</sub> emission. This is the main novelty of this work. In this work, an optimisation framework from (Ibrahim et al., 2018) is extended for such optimal design using machine learning techniques. The ANN models are established to predict TAC, hydrogen production rate and molten salt heat duty in SSMR-MS. A linear regression model is also developed to describe the relationship between solar equipment cost and molten salt duty using System Advisor Model (SAM) (NREL., 2015). Based on these, a surrogate model-based optimisation problem incorporating the proposed ANN models and linear regression model for integration of the entire SSMR-MS and the solar cost is developed. A hybrid global optimisation algorithm is employed to solve the developed optimisation problem and generate the optimal design, which is then validated in Aspen Plus V8.8 and SAM. Besides the process option from (Likkasit, 2015), three novel options in the SSMR-MS are proposed and investigated. The computational results demonstrate that when the pre-reformer is an adiabatic reactor, the best TAC can be generated. As a result, a significant reduction in TAC by 14.90 % ~ 15.10 % and CO<sub>2</sub> emissions by 4.36 % ~ 5.23 % can be achieved compared to the existing SSMR-MS. The molten salt duty is reduced from 20 MW to 10.20 ~ 10.32 MW, resulting in a decrease of the solar field equipment cost by approximately 28.64 %.

## 2. Problem description

Figure 1 illustrates a schematic diagram of the SSMR-MS process for large-scale hydrogen production. Treated natural gas and steam is heated to approximately 400 °C and fed into a pre-reformer where the reactions of steam methane reforming take place. The pre-reformer can be adiabatic or non-adiabatic. If non-adiabatic, molten salt transfers concentrated solar energy in heat to pre-reformer. The flow scheme in the pre-reformer can be co-current or counter-current. The pre-reformer effluent goes into a reformer where the reactions of steam methane reforming occur at high temperature (e.g., 900 °C). The energy required in the reformer is provided through combustion of natural gas with air. The syngas produced in the reformer is cooled down and fed into water gas shift reactors in series. In these two shift reactors, water-gas shift reaction takes place which converts carbon monoxide into hydrogen to improve the productivity of hydrogen. After that, the hydrogen-rich syngas stream is sent for water and CO<sub>2</sub> removal. A pressure swing adsorption (PSA) unit is then used to purify the hydrogen product stream. The off-gas from PSA containing unreacted CH<sub>4</sub>, CO, and leftover H<sub>2</sub>, is recycled back as a fuel for providing heat to the reformer. The process is to produce  $F_{H_2}$  hydrogen with  $\eta_{H_2}$  purity to satisfy hydrogen demand in an oil refinery.

The reactions occurring in the pre-reformer and reformer reactors are shown in Eqs(1)-(3). An Ni-based catalyst is normally used for steam methane reforming. The reaction occurring in the two water gas shift reactors is Eq(2).

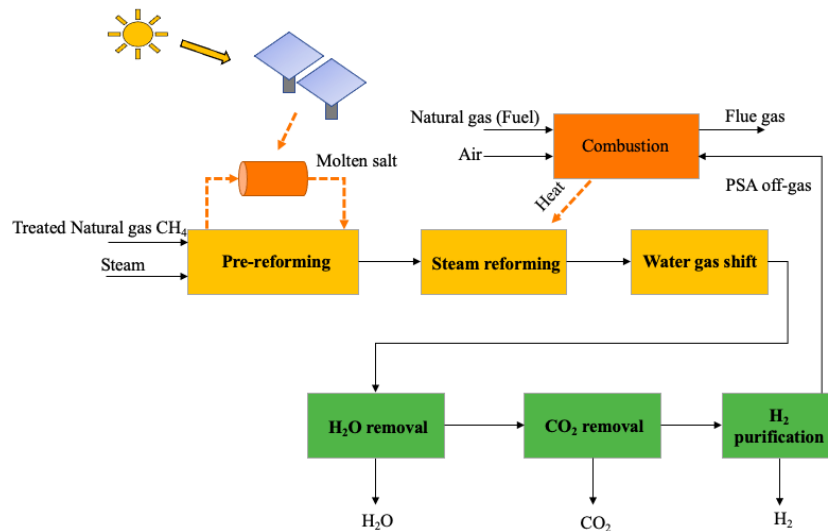


Figure 1: Block diagram of the SSMR-MS process (Modified from Likkasit, 2015)

Given the necessary data including production requirements, reactor types, flow scheme, reaction kinetics, thermodynamic data and economic correlations, the entire problem is to determine optimal operating conditions including stream flowrates, temperature, steam to methane (S/C) ratio, reactor sizes including tube length and tube number as well as optimal heat exchanger network. The objective is to minimise TAC.

## 3. Mathematical formulation

The SSMR-MS process can be modelled using rigorous models in Aspen Plus V8.8. Such rigorous models include mass and energy balance equations, thermodynamic relations, and properties equations, which are often highly complex. The optimisation problem using these rigorous models is denoted as P. To reduce the complexity of the problem P, a surrogate model based on machine learning techniques is developed for the entire SSMR-MS through extending the optimisation framework of Ibrahim et al. (2018). In other words, the whole SSMR-MS process is considered as a black box. There are usually three steps for the development of a

surrogate model, including data generation (i.e., sampling), construction of the surrogate model and construction of feasibility constraints using a support vector machine (Ibrahim et al., 2018).

### 3.1 Data generation

To develop a surrogate model, the first step is data generation because the prediction accuracy of the surrogate model strongly relies on the quality of the data used in the training stage. In this work, input variables including molar flowrate of natural gas into pre-reformer  $F_{NG}$ , steam to methane ratio  $\gamma_{S/C}$ , operating temperature of reformer  $T_R$ , high-temperature water gas shift (HWGS) reactor  $T_{HWGS}$ , low-temperature water gas shift (LWGS) reactor  $T_{LWGS}$ , tube length of pre-reformer  $L_{PR}$ , reformer  $L_R$ , HWGS reactor  $L_{HWGS}$  and LWGS reactor  $L_{LWGS}$ , tube number in pre-reformer  $N_{PR}$ , reformer  $N_R$ , HWGS reactor  $N_{HWGS}$  and LWGS reactor  $N_{LWGS}$  vary between lower and upper bounds. A vector  $\mathbf{x}$  is used to denote all these variables. In other words,  $\mathbf{x} = [F_{NG}, \gamma_{S/C}, T_R, T_{HWGS}, T_{LWGS}, L_{PR}, L_R, L_{HWGS}, L_{LWGS}, N_{PR}, N_R, N_{HWGS}, N_{LWGS}]$ . Then:

$$x^L \leq \mathbf{x} \leq x^U \quad (4)$$

The output variables include TAC, hydrogen production rate  $F_{H_2}$  and molten salt duty  $Q_{MS}$ . Samples generated using the Latin hypercube sampling method are used as input in Aspen Plus V8.8 to get values for the corresponding output variables.

### 3.2 Construction of surrogate models

ANN is used to create a surrogate model of the entire process. A major advantage of ANN over other statistical techniques is the ability to correlate multiple inputs to multiple outputs, leading to compact models that can be implemented in an optimisation environment with ease (Ibrahim et al., 2018). While TAC,  $F_{H_2}$  and  $Q_{MS}$  are correlated with all independent variables using ANN, the relationship of solar-related equipment cost, and molten salt duty is described using algebraic linear function. The  $F_{H_2}$  and purity  $\eta_{H_2}$  are considered as constraints which are indicated below,

$$F_{H_2}^L \leq F_{H_2} \quad (5)$$

$$\eta_{H_2}^L \leq \eta_{H_2} \quad (6)$$

The objective function is to minimise TAC, which can be calculated as follows,

$$TAC = C_{capital} \cdot ACCR + C_{production} \quad (7)$$

where  $C_{capital}$  is total capital investment.  $ACCR$  is annual capital charge ratio.  $C_{production}$  is the total production cost per year.  $ACCR$  is calculated using Eq(8) below,

$$ACCR = [i \times (1 + i)^n] / [(1 + i)^n - 1] \quad (8)$$

where  $i$  is the interest rate per year and  $n$  is the plant lifetime.

The optimisation problem using the surrogate models is stated as follows,

$$\begin{aligned} \text{(PS)} \quad & \text{Min} \quad TAC = TAC_1 + TAC_{solar} \\ & \text{s.t.} \quad TAC_1 = ANN_1(x_I) \\ & \quad \quad TAC_{solar} = f(Q_{MS}) \\ & \quad \quad F_{H_2} = ANN_2(x_I) \\ & \quad \quad Q_{MS} = ANN_3(x_I) \\ & \quad \quad \text{Eqs (4)-(8)} \end{aligned}$$

where  $TAC_1$  is non-solar related cost,  $TAC_{solar}$  is the solar related cost,  $x_I$  is the set of independent variables,  $Q_{MS}$  is molten salt duty. The surrogate model comprises 3 artificial neural networks ( $ANN_1(x_I)$ ,  $ANN_2(x_I)$ ,  $ANN_3(x_I)$ ) and a linear regression model  $f(Q_{MS})$ .

Levelised cost of Hydrogen Production is applied to evaluate the cost for producing one kilogram of hydrogen for one technology within the plant lifetime, as shown in Eq(9) below,

$$LCHP(\$ kg^{-1}) = \left[ \sum_{y=1}^n \frac{(C_{capital} + C_{production})}{(1 + r)^{y-1}} \right] / (m_{H_2} \cdot 8,000 \cdot n) \quad (9)$$

where  $m_{H_2}$  is mass flow rate of hydrogen per hour.

#### 4. Solution algorithm

A hybrid optimisation algorithm similar to that of (Al Jamri et al., 2020) is employed to solve the optimisation problem PS. This hybrid algorithm combines the advantages of the stochastic optimisation algorithm and the deterministic optimisation method. Stochastic optimisation method genetic algorithm (GA) is an evolution-based optimisation method, and it can search the solution space with multiple initial points which increases the possibility to get solution nearby global optimal. Therefore, GA is used to obtain a good feasible initial solution for the problem PS. Then, a deterministic method namely Successive Quadratic Programming (SQP) is used to improve the quality of the feasible solution obtained by GA. The whole optimisation methodology is illustrated in Figure 2. The hybrid solution algorithm is implemented in MatLab R2019a. GA available in the global optimisation toolbox in MatLab R2019a ('ga') is employed.

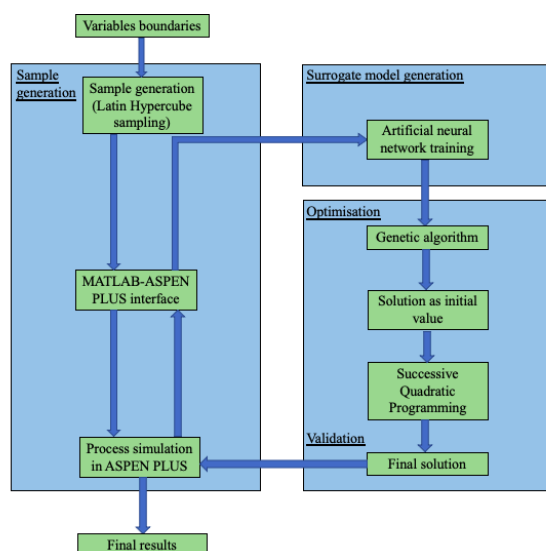


Figure 2: Flowchart of the extended design methodology

#### 5. Computational studies

The extended optimisation approach is used to generate the optimal design of the SSMR-MS process. The hydrogen production rate is 2,577 kmol h<sup>-1</sup>. The desired hydrogen purity is 99.9 vol%. As discussed in the problem statement, there are four options that should be investigated in the SSMR-MS. In the first option, the pre-reformer is considered as a non-adiabatic reactor. Its energy is supplied by molten salt with a co-current flow regime. The process with this option is denoted as SSMR-MS-1. This SSMR-MS-1 process is exactly the same as that in (Likkasit, 2015). In the second option, the pre-reformer is considered as a non-adiabatic reactor whose energy supplied by molten salt with a counter-current flow scheme. The resulting process is denoted as SSMR-MS-2. In the third option, the pre-reformer is considered as an adiabatic reactor. Molten salt is used to heat the inlet streams natural gas and steam. The resulting process is defined as SSMR-MS-3. In the last option, the pre-reformer and two water gas shift reactors are considered as adiabatic reactors where molten salt provides heat to the process similar in SSMR-MS-3. This option is denoted as SSMR-MS-4.

Four process options are modelled using Aspen Plus V8.8 and a 'base case' simulation of each SSMR-MS process is developed based on data from Likkasit (2015). The thermodynamic property method PENG-ROB is selected due to its suitability to organic products and hydrogen gas (Özcan et al., 2019). The results obtained from the 'base case' simulation of SSMR-MS-1 indicate that the TAC is 143.8 M\$ yr<sup>-1</sup>, which is quite close to the TAC of 144.0 M\$ yr<sup>-1</sup> in (Likkasit, 2015) with the deviation within 0.13 %.

The optimisation problem PS is solved for each SSMR-MS process option using the hybrid optimisation algorithm. The results are given in Table 1. The optimal values of independent variables in Table 1 are used as input in Aspen Plus V8.8 to generate values of all dependent variables and update  $Q_{MS}$ ,  $F_{H_2}$  and TAC. The updated results are provided in Table 2. From Table 1 and Table 2, it can be seen that the largest difference between actual results and prediction results from the ANN surrogate model is within 1 %. The largest difference for molten salt heat duty is only 0.05 %. For instance, actual optimal TAC in SSMR-MS-2 is 136.55 M\$ yr<sup>-1</sup>, which is only 0.58 % difference compared to the predicted TAC of 135.76 M\$ yr<sup>-1</sup>. These demonstrate that the ANN surrogate model has high prediction accuracy. The results obtained from the extended optimisation

framework are also validated using the hybrid feasible path optimisation algorithm from (Ma et al., 2020) and (Ma et al., 2021), which is employed to solve the original problem P directly. The largest difference is 0.30 %, which further demonstrates the effectiveness of the extended optimisation-based framework.

Table 1: Optimisation results for SSMR-MS-1, SSMR-MS-2, SSMR-MS-3, SSMR-MS-4 from surrogate models

Item	Initial value	SSMR-MS-1	SSMR-MS-2	SSMR-MS-3	SSMR-MS-4
$\gamma_{S/C}$	4	2.0	2.0	2.0	2.0
$T_R$ (°C)	900	995.9	991.6	993.3	996.9
$T_{HWGS}$ (°C)	400	352.1	372.1	446.1	401.7
$T_{LWGS}$ (°C)	200	209.4	197.5	206.7	208.3
$L_{PR}$ (m)	6.1	11.0	11.1	11.1	11.1
$L_R$ (m)	10	10.1	10.3	11.4	11.5
$L_{HWGS}$ (m)	6.1	4.5	4.6	4.7	4.7
$L_{LWGS}$ (m)	6.1	3.8	3.9	3.9	3.9
$N_{PR}$	12,500	4,006	4,010	4,000	4,000
$N_R$	135	51	56	50	50
$N_{HWGS}$	2,000	1,002	1,221	3,000	1,000
$N_{LWGS}$	3,250	2,282	2,214	2,000	4,000
$F_{NG}$ (kmol h <sup>-1</sup> )	778.3	799.7	803.7	803.3	812.9
$Q_{MS}$ (MW)	20	12.37	12.89	10.25	10.34
$F_{H_2}$ (kmol h <sup>-1</sup> )	2,577	2,577	2,577	2,577	2,577
TAC (M\$ yr <sup>-1</sup> )	159.37	134.88	135.76	131.86	131.96

Table 2: Updated results for SSMR-MS-1, SSMR-MS-2, SSMR-MS-3, SSMR-MS-4 using Aspen Plus V8.8

Item	SSMR-MS-1		SSMR-MS-2		SSMR-MS-3		SSMR-MS-4	
	Base	Optimal	Base	Optimal	Base	Optimal	Base	Optimal
	Case	Case	Case	Case	Case	Case	Case	Case
$Q_{MS}$ (MW)	20	12.35	21	12.84	17	10.20	19	10.32
$F_{H_2}$ (kmol h <sup>-1</sup> )	2,577	2,577.1	2,577	2,578.3	2,577	2,577.3	2,577	2,577.1
TAC (M\$ yr <sup>-1</sup> )	144.0	136.21	148.6	136.55	141.9	133.11	145.8	131.95
TAC with heat integration (M\$ yr <sup>-1</sup> )	144.0	128.4	148.6	125.7	141.9	122.2	145.8	122.5
LCHP (\$ kg <sup>-1</sup> )	2.85	2.52	2.90	2.45	2.81	2.43	2.87	2.43

Table 3: Optimal design of the solar field for SSMR-MS-1, SSMR-MS-2, SSMR-MS-3 and SSMR-MS-4

Item	SSMR-MS-1		SSMR-MS-2		SSMR-MS-3		SSMR-MS-4	
	Base	Optimal	Base	Optimal	Base	Optimal	Base	Optimal
	Case	Case	Case	Case	Case	Case	Case	Case
$Q_{MS}$ (MW)	20	12.35	21	12.84	17	10.20	19	10.32
Solar tower height (m)	98.08	69.49	90.80	71.71	95.23	90.15	86.53	67.39
Heliostat reflective area (m <sup>2</sup> )	83,303	52,333	88,688	53,859	71,094	42,369	78,096	43,895
Receiver area (m <sup>2</sup> )	130.49	121.28	154.43	117.52	121.23	99.84	141.69	95.95
Receiver thermal capacity (MW)	50.00	30.87	52.50	32.09	42.50	25.00	47.50	25.80
Storage capacity (MW)	300.00	185.23	315.00	192.54	255.00	150.00	285.00	154.79
Land area (acres)	121	107	135	107	109	81	127	93

To further reduce the operation cost, heat integration is conducted for the optimal SSMR-MS-1, SSMR-MS-2, SSMR-MS-3 and SSMR-MS-4, respectively. The results are illustrated in Table 2. From Table 2, it can be seen that after heat integration, the TAC is reduced by 10.80 %, 15.45 %, 13.85 %, and 15.86 % for SSMR-MS-1, SSMR-MS-2, SSMR-MS-3 and SSMR-MS-4, respectively. SSMR-MS-3 and SSMR-MS-4 have the lowest LCHP of 2.43 \$ kg<sup>-1</sup>, which is reduced by around 14.74 % compared to that of the existing process. SSMR-MS-2 with LCHP at 2.45 \$ kg<sup>-1</sup> is only slightly higher than those two optimal designs. With the price of per unit hydrogen cost decrease, SSMR-MS process has a greater potential to be applied to large-scale hydrogen production. Optimal molten salt duty is sent as an input in SAM to generate the optimal design of the solar field. The results are provided in Table 3. With a significant reduction in molten salt heat duty, heliostat reflective area, receiver area, receiver thermal capacity, storage capacity and land area also decrease significantly.

Table 4 provides comparative results of SSMR-MS-3 and SSMR-MS-4 with those of conventional steam reforming of natural gas (SMR) from (Likkasit, 2015). From Table 4, it can be seen that, with around 12 % reduction in natural gas consumption and over 60 % reduction in electricity consumption in SSMR-MS-3 and SSMR-MS-4 than that in SMR, the energy efficiency is improved by around 12.08 % and 14.18 % in SSMR-MS-3 and SSMR-MS-4. CO<sub>2</sub> emission in SSMR-MS-3 and SSMR-MS-4 reduces around 80 kt yr<sup>-1</sup>, compared to that in SMR. Although TAC of SSMR-MS-3 and SSMR-MS-4 is significantly reduced after optimisation, compared to the existing SSMR-MS, their TAC is still higher than that of SMR due to high solar-related equipment cost. As a result, the LCHP of SSMR-MS-3 and SSMR-MS-4 is still 0.41 \$ kg<sup>-1</sup> higher than that of SMR. If carbon tax and additional credit can be supplied for the use of solar energy from the government, the optimal SSMR-MS-3 and SSMR-MS-4 could be competitive to SMR for large-scale hydrogen production.

Table 4: Comparative results for SMR, SSMR-MS-3 and SSMR-MS-4

	SMR	SSMR-MS-3	SSMR-MS-4
Natural gas consumption (kt yr <sup>-1</sup> )	150.25	132.85	132.12
Water consumption (kt yr <sup>-1</sup> )	453.17	552.13	555.15
Electricity consumption (GWh yr <sup>-1</sup> )	93.51	33.39	29.64
CO <sub>2</sub> emissions (kt yr <sup>-1</sup> )	502.93	423.85	420.00
Energy efficiency (%)	62.99	70.60	71.92
TAC (M\$ yr <sup>-1</sup> )	90.9	122.2	122.5
LCHP (\$ kg <sup>-1</sup> )	2.02	2.43	2.43

## 6. Conclusions

In this paper, the optimisation-based framework using machine learning techniques is extended for optimal design of SSMR-MS for large-scale hydrogen production. Four different process options in SSMR-MS have been investigated. The computational results show that TAC was reduced by up to 15 % compared to the existing SSMR-MS process. The molten salt heat duty was reduced from 20 MW to 10.20 MW. Although the extended framework can be used to generate the optimal design, it cannot theoretically guarantee global optimality. In addition, the lowest LCHP of SSMR-MS-3 and SSMR-MS-4 is still 0.41 \$ kg<sup>-1</sup> higher than that of SMR. Therefore, the future work is to investigate different carbon utilization methods to further reduce TAC and LCHP.

## References

- Al Jamri, M., Li, J., Smith, R., 2020, Molecular Modeling of Coprocessing Biomass Fast Pyrolysis Oil in Fluid Catalytic Cracking Unit, *Industrial & Chemistry Engineering Research.*, 59,1989-2004.
- Hydrogen Council., 2017, Hydrogen Scaling up: a Sustainable Pathway for the Global Energy Transition.
- Ibrahim, D., Jobson, M., Li, J., Guillén-Gosálbez, G., 2018, Optimization-based design of crude oil distillation units using surrogate column models and a support vector machine, *Chemical Engineering Research & Design.*, 134, 212-225.
- Koumi Ngoh, S., Njomo, D., 2012, An overview of hydrogen gas production from solar energy, *Renewable and Sustainable Energy Reviews*, 16, 6782-6792.
- Likkasit, C., 2015, Integration of renewable energy to oil and gas industry: solar-aided hydrogen production. King Mongkut's University of Technology Thonburi, Bangkok, Thailand.
- Liu, G., Sheng, Y., Ager, J. W., Kraft, M., Xu, R., 2019, Research advances towards large-scale solar hydrogen production from water, *EnergyChem*, 1, 100014.
- Ma, Y., McLaughlan, M., Zhang, N., Li, J., 2020, Novel feasible path optimisation algorithms using steady-state and/or pseudo-transient simulations, *Computers & Chemical Engineering*, 143, 107058.
- Ma, Y., Zhang, N., Li, J., Cao, C., 2021, Optimal design of extractive dividing-wall column using an efficient equation-oriented approach, *Frontiers of Chemical Science and Engineering*, 15, 72-89.
- National Renewable Energy Laboratory (NREL). System Advisor Model (SAM 2015.01.30). accessed 05.04.2021.
- Özcan, O., Akin, A. N., 2019, Thermodynamic analysis of methanol steam reforming to produce hydrogen for HT-PEMFC: An optimization study, *International Journal of Hydrogen Energy*, 44, 14117-14126.
- Turner, J., Sverdrup, G., Mann, M. K., Maness, P.-C., Kroposki, B., Ghirardi, M., Evans, R. J. & Blake, D., 2008, Renewable hydrogen production, *International Journal of Energy Research*, 32, 379-407.
- Voldsund, M., Jordal, K., Anantharaman, R., 2016, Hydrogen production with CO<sub>2</sub> capture, *International Journal of Hydrogen Energy*, 41, 4969-4992.